10th International Federation of Automatic Control (IFAC) World Congress
München, Juli 1987
Preprints

AUTONOMOUS HIGH SPEED ROAD VEHICLE GUIDANCE BY COMPUTER VISION*

E.D. Dickmanns
A. Zapp

Aerospace Engineering Department, Universität der Bundeswehr München, Neubiberg, FRG

Abstract. A visual feedback control system has been developed which is able to guide road vehicles on well structured roads at high speeds. The road boundary markings are tracked by a multiprocessor image processing system using contour correlation and curvature models together with the laws of perspective projection. Feature position data are the input into Kalman filters to estimate both the vehicle state vector relative to the driving lane and road curvature parameters. Velocity is measured conventionally. Longitudinal control by throttle and braking is geared to lateral acceleration due to road curvature; lateral control has an anticipatory feed forward and a compensatory feedback component. The control system has been tested with a CCD TV-camera and image sequence processing hardware in a real time simulation loop and with our experimental vehicle, a 5 ton-van equipped with sensors, onboard computers and actuators for autonomous driving.

Keywords. Automatically guided vehicles; Computer vision; Multiloop feedback control; Multiprocessors; Knowledge based control.

1. INTRODUCTION

With the substitution of animals towing carriages by engines on the vehicle, engineering opened up a new aera of transportation. On the one hand this brought about new ranges of speed and mobility but on the other hand it necessitated the continuous attention of a driver to control the vehicle. A horse is able to learn the way it is being guided (e.g. in the middle of the right half of a road) and the road system around its home; so it is able to at least partially navigate correctly in a known environment. In addition, trained horses can take oral commands like which way to take at a road junction. The (of course limited) autonomous capabilities, which the trained animal provided using its visual and auditory senses and the brain behind it have been traded for the performance advantages of the auto-mobile.

The highly integrated electronic devices of the near future may allow regaining and even improving the sacrificed capabilities for modern high performance vehicles. High frequency image sequences (like TV-signals) and auditory inputs can be analysed by computers to allow autonomous vehicle guidance. At present this is possible only in a simple way but this will change with the highly parallel VLSI systems to come.

Investigations into autonomous vehicle guidance have been performed for some time. Systems using special installations along the road like beacons or buried wires are not considered here; they do not allow to detect obstacles, neither near the vehicle nor in anticipation along the road. This capability to detect the actual state of the environment and to check the viability of locomotion is considered to be a main ingredient for autonomous driving in the sense adopted here.

The planetary rover of NASA [Gennery, 1977] probably was the first project to spur serious research in this field for some time. Most of the other systems investigated in the 70ies were laboratory carts of small size and low speed that were able to move only intermittently, either measuring or moving (for a survey see [Giralt, 1984]). Pioneering work in this field has been done by Moravec [Moravec, 1980]. A new drive towards real applications originated from the US-DARPA Program on Strategic Computing, in which the Autonomous Land Vehicle (ALV) has been selected as one of the demonstrator projects [IRD, 1985]. Road following at low speeds was defined as an initial goal and has been achieved in 1985 [AWS, 1986]; the goal of the project is to achieve the capability of autonomous cross-country mobility.

In contrast, the research reported on here aims at providing the capability of autonomously guiding a high speed vehicle along a well structured, normed, limited access highway with one way traffic, no crossings and a limited class of participants (e.g. Autobahn). This puts relatively low requirements on image processing and yet is possibly of practical importance (autopilot). With the advent of more powerful miniaturized computer systems this may even become economically viable for general traffic applications. Future growth potential exists in the direction of autonomous mobility in more complex environments like state, country and eventually city road nets. The system is intended to fit into the present traffic situation with its rules and regulations, requiring no additional installations along the road network and allowing a smooth, gradual deployment (like autopilots in aviation). Like these it is conceived as an add on option to driver control systems.

2. SYSTEM CONCEPT

A system for autonomous mobility on roads has to provide at least the following 5 functions (for more details see [Dickmanns, 1986a]):

1. Detection of the road and its parameters like curvature, lane width, surface state, presence or absence of obstacles (static objects).

*The research reported here has been partially supported by the Fed. Ministry of Research and Technology (BMFT) of the FRG.

2. Recognition of relative position in the lane and of position and speed relative to other moving objects.
3. Correct interpretation of traffic information like road markings (e.g. lines, interupted or not), traffic signs (e.g. speed limits) and local warnings.
4. Safe and efficient control of the vehicle depending on the actual state resulting from 1 to 3 above.
5. Easy human interface for both switching from human to autonomous control and back and for human decision taking on request of the automatic system (warning functions).

The sensory unit of the experimental system under development consists of two black and white CCD TV-cameras, mounted on a fast pointing device, inertial sensors like angular rate and linear acceleration detectors and conventional sensors for speed and control actuator positions. One of the cameras has a wide angle field of view, the other a tele lens for good resolution farther away in order to achieve good look ahead performance. The signals of both cameras are digitized into 256*256*8 bit data streams which are given onto two digital video buses of the image processing system BVV (fig. 1).

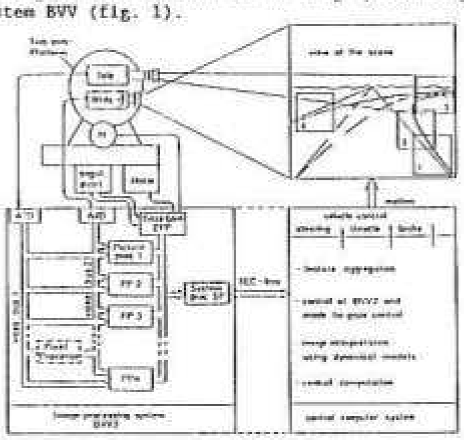

Fig. 1. Block diagram of image processing system BVV and visual control loop

Selected rectangular subareas of these images, called windows, are analysed by this multimicroprocessor system developed by V. Graefe and coworkers [Graefe, 1984]. The image processing is described in the next section.

Interpretation and control of the image processing is performed by the main computer, in which knowledge about the process to be controlled is coded. This processor fuses the information derived from images with that coming from other sensors and computes the controls for the vehicle exploiting a dynamical world model. It also determines the mode of operation of the BVV and the pointing system. The basic digital control cycle is 5 (60 Hz-) video cycles (83 ms).

3. INTEGRATED APPROACH FOR IMAGE SEQUENCE PROCESSING, STATE ESTIMATION AND CONTROL

3.1 The image processing system BVV

The image processing system (fig. 1) has been developed as a flexible tool for performing research into basic algorithms and architectures for real time image sequence analysis with easily available technology. It allows up to 14 parallel processors (PP) to get access to digitized images, from which each one takes that part it happens to be interested in. Whithin its window the processor looks for special features, usually a collection of line elements detected by correlation methods with ternary masks [Kuhnert, 1985], and reports their position and slope to a hierarchically higher ranked processor which is not necessarily the main computer. This one tries to aggregate the results of several PP in order to recognise the perspective projection of a known object in the 3D world. If it is successfull it orders the PP to independently track its feature over the image sequences; windows of several PP may move freely over the entire image area and overlap without memory access interference. Functional parallelism may be obtained by having PP's investigate the same image area with different algorithms. If one interpreting processor receives information contradicting its actual world model, it can redirect a PP to a new image area, where a feature is supposed to be visible in support of the object hypothesis being persued. Thus, a hypothesis may either have to be abandoned or may become a stable interpretation of the image sequence yielding the state of the vehicle relative to the road.

For the road scene shown in the upper right part of fig. 1 the interpretation proceeds as follows: At first, assuming the vehicle is on a road, the right lane marking in the close up vicinity of the vehicle is looked for. If the viewing direction is approximately tangential to the road and the lane markings satisfy continuity conditions (equal width, smoothly changing direction and small curvatures), this lane marking appears in the lower right part of the image as an almost straight line inclined to the left at an angle depending on the elevation h of the camera above the ground and on the distance d of the camera to the left of the line. For a given vehicle/camera configuration the proper position of this line in the field of view for correct lane following is known from perspective projection. Deviations from this due to position and heading errors of the vehicle are used as compensatory contributions to the steering control applying a linear feedback law [Dickmanns, 1985].

The extrapolation of this line towards the horizon gives the reference for the detection of road curvature. If a planar environment is assumed the relative positions of the measured lane markings in greater look ahead distances immediately give the sign of the curvature. If both vertical and horizontal curvatures are allowed, two lane markings have to be tracked and extrapolated in order to resolve the horizontal and vertical components of the curvature seperately. In order to check the state of the road surface, much more involved image processing is needed.

3.2 Road model and transformation for recursive estimation

Here, only those parts necessary for guiding the vehicle along a lane are given, omitting other objects and traffic information. High speed roads are modelled as a sequence R of N arcs with linear curvature models defining the skeleton of a band with constant width b.

$$R = \sum_{i=1}^{N} (C_{oi} + C_{1i} l_i) \; ; \quad 0 \le l_i \le \lambda_i \qquad (1)$$

C_o is the constant curvature part of the model and $C_1 = dC/dl$ is the linearly variing part over arc length. The parameters of this structural model (C_{oi}, C_{1i} and λ_i) have to be determined from the visual input for a certain range L in front of the vehicle. The curvature C is used both for longitudinal control (of speed) and for the feed forward contribution to the lateral control (steering).

Moving at speed V along the road, the curvature changes C(l) appear in the image plane of the camera as time varying curves. Therefore, exploiting eq. (1) and the relationship V = dl/dt, a simple dynamical model for the road image change while driving along the road can be given. For an eye-point at the elevation h above the road and $b/2 \cdot y_v$ from the right border line, where b/2 is the lane width and y_v the lateral position off the lane center, a line element of the border line at the look-ahead distance L is mapped onto the image plane y_B, z_B according to the laws of perspective projection (see fig. 2)

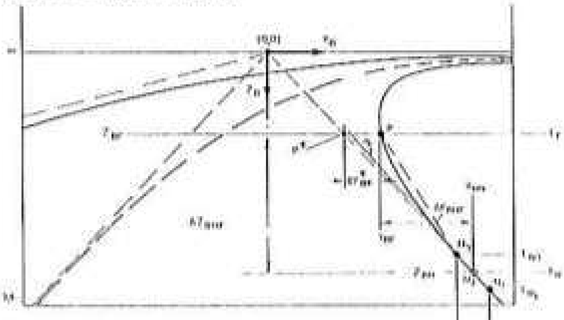

Fig. 2. Symbols for planar curvature analysis

P^* would be the image point for a straight planar road with $y_v = 0$ and the camera looking parallel to the road. A road curvature according to an element of eq (1) would yield the lateral offset y_C from the straight line by integrating eq (1) twice with respect to arc length (approximating the sine by its argument, for details see [Dickmanns, 1986b]) at the look-ahead distance L:

$$y_C \approx C_o L^2/2 + C_1 L^3/6 \tag{2}$$

Fig. 3 shows the more general situation in a top-down view where both a lateral offset y_v and a nontangential viewing direction ψ_K yielding an offset $L\psi_K$ have been added, all of which contribute to a shift of the image points P and P^*. Perspective projection onto a focal plane at distance f yields for the image coordinates

$$y_B = f(b/2 - y_v + y_C - L\psi_K)/L; \quad z_B = fh/L \tag{3}$$

With $\quad y_L = Ly_B/f = b/2 - y_V + y_C - L\psi_K \qquad (4)$

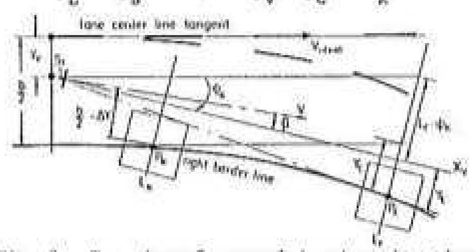

Fig. 3. Top view of general imaging situation with lateral offset y_v, nontangential viewing direction ψ_K and road curvature (y_C); two preview ranges L_N and L_F

as an intermediate variable, a dynamical model for road curvature determination is obtained by taking the time derivative and introducing substitutions:

$$\dot{y}_L = -\dot{y}_V + \dot{y}_C - L\dot{\psi}_K \tag{5}$$

The lateral speed $\dot{y}_v$ relative to the road may be expressed by the relative path angle $\Delta\chi$ between vehicle velocity vector $\underline{V}$ and road tangent. Assuming that the viewing direction is fixed to the car body axis, the side slip angle β between $\underline{V}$ and ψ_K has to be taken into account yielding

$$\dot{y}_v = V\Delta\chi = V(\psi_K - \beta) . \tag{6}$$

For the term $\dot{y}_C$ one obtains form eq (2), shifting the reference point from l = 0 to l = L, since the measurements are taken there, and naming the corresponding curvature state at the vehicle location C_{oL},

$$\dot{y}_C = \frac{d}{dt} (C_{oL} - 2C_1 L/3)L^2/2 .$$

By definition of the road model eq (1) using the chain rule there follows

$$\frac{d}{dt}(C_{oL}) = \frac{d}{dl}(C_{oL})\frac{dl}{dt} = C_1 V \tag{7}$$

$$\dot{C}_1 = \frac{d}{dt}(C_1) = \begin{cases} 0 & \text{on one segment} \\ V\delta(l-\lambda_i), & \text{a Dirac-impulse} \end{cases} \tag{8}$$

at a transition point λ_i; for practical purposes C_1 is considered to be Gaussian random noise w(t).

The term $\dot{\psi}_K$ in eq (5) is the inertial vehicle yaw rate $\dot{\psi}_v$ minus the heading change of the road over time, which is curvature times speed

$$\dot{\psi}_K = \dot{\psi}_v - C_{oL} V . \tag{9}$$

Eqs (5) to (9) yield the state space model for road curvature estimation

$$\begin{bmatrix} \dot{y}_L \\ \dot{C}_{oL} \\ \dot{C}_1 \end{bmatrix} = \underbrace{\begin{bmatrix} 0 & LV & L^2V/2 \\ 0 & 0 & V \\ 0 & 0 & 0 \end{bmatrix}}_{\underline{A}_R} \begin{bmatrix} y_L \\ C_{oL} \\ C_1 \end{bmatrix} + \begin{bmatrix} -L & V & -V \\ 0 & 0 & 0 \\ 0 & 0 & 0 \end{bmatrix} \begin{bmatrix} \dot{\psi}_v \\ \beta \\ \psi_K \end{bmatrix} + \begin{bmatrix} 0 \\ 0 \\ w(t) \end{bmatrix} \tag{10}$$

3.3 Vehicle model

The experimental vehicle available (named VaMoRs), is an especially equipped 5-ton van DB 508D with an automatic 4 gear change and a rear axle drive (see fig. 4). Total mass is $m \approx 4000$ kg with the center of gravity (c.g.) at 2.0 m behind the front

Fig. 4. The experimental vehicle VaMoRs

axle of the wheel base of 3.5 m and about 0.7 m above the ground. The effective wheel radius is $r \approx 0.36$ m. The engine power is 63 KW which, considering the tractional resistances yields a maximum speed of about 100 km/h. This means, that the controllers have to be designed for the speed range $0 < v \leq 30$ m/s.

3.3.1 Longitudinal dynamics

According to [Mitschke, 1982] the following equation is used for describing the longitudinal acceleration:

$$\dot{V} = \frac{1}{m \cdot r \cdot \eta} \cdot [i_g \cdot M_{mot}(\omega_{mot}, \varphi_{thr}) - M_{res}] , \tag{11}$$

where i_g is the ratio of the gearing and the rear axle, and η is a factor taking the inertia of the rotary parts of the engine and the gearing into account. The engine torque M_{mot} is a function of the engine speed ω_{mot} and the throttle position φ_{thr}; M_{res} comprises the different tractional resistances like air drag, rolling friction, braking friction and resistance in curves.

3.3.2 Lateral dynamics

A planar 'bicycle' substitution model according to [Strackerjan, 1975] has been applied. Its two degrees of freedom are the sideslip angle β and the inertial yaw rate $\dot{\psi}_V$ described by the following equations of motion:

$$mV\dot{\beta} + (U_f + U_r + \mu c_f + \mu c_r)\beta - (mV + \mu c_f \frac{l_f}{V} - \mu c_r \frac{l_r}{V})\dot{\psi}_V = -(U_f + \mu c_f)\delta \tag{12}$$

$$I_z \ddot{\psi}_V + \frac{\mu}{V}(c_f l_f^2 + c_r l_r^2)\dot{\psi}_V - \mu(c_f l_f - c_r l_r)\beta = (U_f l_f + \mu c_f l_f)\delta \tag{13}$$

where I_z is the moment of inertia around the vertical axis, $c_{f,r}$ are normal side force coefficients applicable to front and rear axles. $l_{f,r}$ are the distances of the c.g. to the front and rear axle respectively, $U_{f,r}$ are the circumferential forces on the wheels and μ is the friction coefficient between wheels and road.

δ is the steer angle of the front wheels. A computer controlled stepping motor serves as actuator for steering. It has been modelled as an integrator

$$\dot{\delta} = k_\delta \cdot u , \tag{14}$$

where $\dot{\delta}$ is limited to 15 degrees/sec.

3.4 Integrated state space model for visual control

Combining eqs (5)(6)(9)(12)(13) and (14) one obtaines a statespace model for lateral dynamics relative to a road with visual measurements taken at the look ahead distance L_N in the near range. It is of fifth order with the state variables $x^T = (\dot{\psi}_V, \beta, \psi_K, \Delta y, \delta)$. Δy in the near look ahead range L_N is defined such that for the reference state the velocity vector is tangential to the road (see fig. 3).

$$\dot{\underline{x}} = \underline{A}_V \underline{x} + \underline{b} u + \underline{g}\, C_{oL} , \text{ where} \tag{15}$$

$$\underline{A}_V = \begin{bmatrix} a_{11} & a_{12} & 0 & 0 & a_{15} \\ a_{21} & a_{22} & 0 & 0 & a_{25} \\ 1 & 0 & 0 & 0 & 0 \\ a_{41} & a_{42} & V & 0 & a_{45} \\ 0 & 0 & 0 & 0 & 0 \end{bmatrix} ; \quad \underline{b} = \begin{bmatrix} 0 \\ 0 \\ 0 \\ 0 \\ 1 \end{bmatrix} ; \quad \underline{g} = \begin{bmatrix} 0 \\ 0 \\ -V \\ LV \\ 0 \end{bmatrix}$$

The components $\dot{\psi}_K$ and $\Delta\dot{y}$ contain a contribution due to road curvature C_{oL}. The elements a_{ij} depend upon the parameters V, m, μ and L.

The dominant effects caused by parameter changes are due to speed variations, which also are the most frequent ones. Adaptations to changes in mass m are - if at all - only necessary at the beginning of a mission. Changes in friction coefficient μ may be due to road surface parameters including wheather conditions. Since speed is the only easily measurable variable and has the largest influence on vehicle behaviour, its effect on the model is always taken into account, i.e. the nonlinear physical model is approximated by a timevarying mathematical model with speed V governing the coefficients [Zapp, 1985]. In VaMoRs speed is derived from the digital odometer system.

The two systems of eqs (10) and (15) may be combined yielding an 8*8 matrix which nicely shown the interactions

$$\left[\begin{array}{ccccc:ccc} & & & & & & 0 & \\ & & & & & & 0 & \\ & & \underline{A}_V & & & \underline{0} & -V & \underline{0} \\ & & & & & & LV & \\ & & & & & & \underline{0} & \\ \hdashline -L_F & V & -V & 0 & 0 & & & \\ & & \underline{0} & & & & \underline{A}_R & \\ & & \underline{0} & & & & & \end{array}\right] \begin{bmatrix} \dot{\psi}_V \\ \beta \\ \psi_K \\ \Delta y \\ \delta \\ y_L \\ C_{oL} \\ C_1 \end{bmatrix} = \underline{A}_t \underline{x}_t . \tag{16}$$

The main diagonal blocks are treated by seperate Kalman filters. The effect of column 7 in the upper right corner is handled seperately as anticipatory part for the lateral control (steer angle to achieve a curved trajectory according to C_{oL}). The effect of the vehicle state on curvature measurement (first line in lower left block) is taken into account by crossfeeding the corresponding estimated variables of the vehicle state vector which are based on visual data from the near field of view into the Kalman filter for road curvature estimation (s. fig. 6 below).

The latter one is a complete filter formulation while for vehicle state estimation a quasi stationary filter with velocity-dependent coefficients is being used. In addition dependencies on other parameters like m and μ may be taken into account. The measured output variables are the borderline positions y_B in the image, corresponding to the near and far window (index N resp. F). The look ahead distances L_N and L_F for a flat road model are directly geared to the vertical position z_B in the image.

$$\begin{bmatrix} y_{BN} \\ y_{BF} \end{bmatrix} = \left[\begin{array}{ccccc:ccc} 0 & -f & 0 & -f/L_N & 0 & 0 & fL_N/2 & 0 \\ 0 & 0 & 0 & 0 & 0 & f/L_F & 0 & 0 \end{array}\right] \begin{bmatrix} \underline{x}_t \end{bmatrix} + \begin{bmatrix} fb/(2L_N) \\ 0 \end{bmatrix} \tag{17}$$

4. CONTROL SYSTEM DESIGN

4.1 Longitudinal control

Besides the usual driver inputs by pedals a stepping motor for activating the throttle and an electrohydraulic unit for the brake, both computer controlled, are provided in the vehicle. As a safety feature the automatic control is switched off as soon as the driver activates one of the pedals.

In curves a recommended value V_c for the vehicle speed can be given by specifying the permissible lateral acceleration a_y.

$$V_c = [a_y / C_{oL}]^{1/2} ; \tag{18}$$

For conventional road vehicles, depending on the surface conditions, a_y is limited to the order of magnitude 1g, but for more agreeable riding comfort values around 0.1g should be chosen. To adjust vehicle speed the following control law for the longitudinal accelerations has been adopted:

$$\begin{aligned} &\text{acceleration: } \dot{V}_+ = k_{ac} V_c (V_c - V) \quad \text{for } V < V_c \\ &\text{deceleration: } \dot{V}_- = k_{dc}\, V (V_c - V) \quad \text{for } V > V_c \end{aligned} \tag{19}$$

From eq (3) the necessary engine torque or braking friction depending on the actual road curvature C_{oL} can be given.

4.2 Lateral control

The design of the digital controller is performed using well known pole assignment methods. Three eigenvalues of the open loop system eq. (15) always are at the origin. The other two mainly depend on the parameter V and are always well damped; only a slight dependence on mass and friction coefficient μ is observed.

Experience has shown that good closed loop control behaviour at modest control activity can be obtained by shifting only the integrator poles and fixing the other ones at their respective open loop location [Drexler, 1986; Zapp, 1985].

The three integrator poles are shifted into the left half plane on rays from the origin as linear functions of the parameter V (speed). For good step response one conjugate pair with damping ratio $\zeta = 1/\sqrt{2}$ has been selected. The proportionality factor for the real pole was chosen to be -0.1, while for the conjugate pair a factor of -0.2 yielded good results over the entire speed range.

The state feedback gains k_i for this pole placement can be well approximated by

$$k_i(v) = p_{io} + p_{i1}V + p_{i2}V^2 \quad . \tag{20}$$

The coefficients p_{ij} depend upon the actual values of m, μ and L for the mission. Fig. 5 shows step responses of the closed loop system for different velocities.

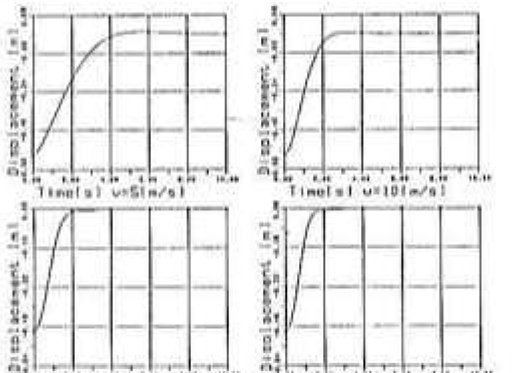

Fig. 5. Step responses of closed loop system for different velocities

The interaction between longitudinal and lateral control based on state estimation by visual measurements may be seen from fig. 6.

5. DISCUSSION OF RESULTS

The system described in the previous sections has been tested in a simulation loop [Dickmanns, 1984] with real image processing hardware included, and with our testvehicle VaMoRs.

5.1 Simulation results

The imaging sensor was a 60 Hz CCD TV-camera Hitachi KP120 mounted in front of a cylindrical projection screen (radius = 2.5 m), onto which the road scene generated by a black and white calli-

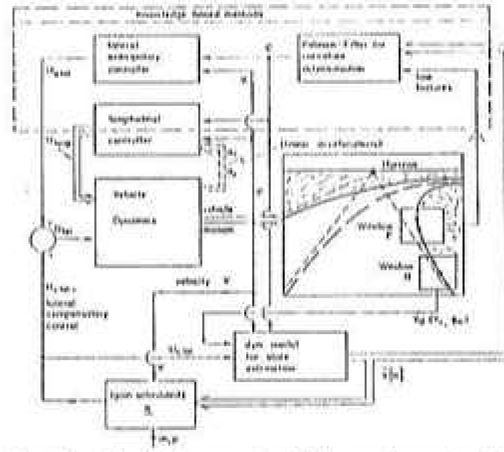

Fig. 6. Block diagram for high speed road vehicle guidance by computer vision.

graphic system was projected. The course to be driven was an eight-shaped slightly hilly course of 1.4 km length and curve radii down to 60 m, which of course is much below Autobahn-standard. Speeds varied between about 30 and 60 km/h and the maximum position offset from the center of the lane was less than 3% of the lane width of 3.25 m, i.e. 9 cm. Due to the curvature feedforward the steady state errors shown in [Dickmanns, 1985] have been eliminated. Figure 7a shows the measured curvatures C(l) together with the computer model C_H for simulation. It is seen that the curvature over the arc length is very well approximated. The remaining errors are compensated by the feedback part of the control u_c. Speed adjustment and the lateral deviations can bee seen from fig. 7b.

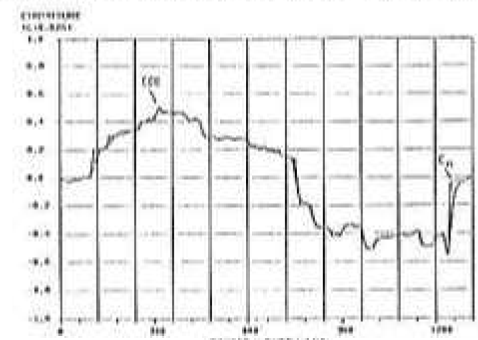

Fig. 7a Simulation result for curvature estimation

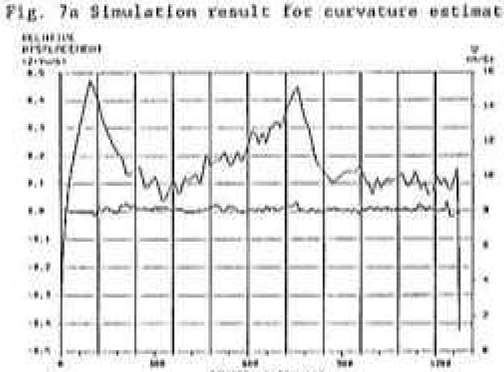

Fig. 7b Vehicle speed and lateral displacement

Fig. 7. Experimental results with real time image sequence processing in a simulation loop including real sensors

5.2 Results with testvehicle VaMoRs

In the last quarter of 1986 VaMoRs became available for autonomous driving tests. The task to be performed is shown in fig. 8. Initially the vehicle is parked at the start position (upper left) in the vicinity of a lane boundary marking according to the German norm. After searching and detecting this line the two real time tracking windows in fig. 1 are positioned in the near and far look ahead range. Then the vehicle starts mov-

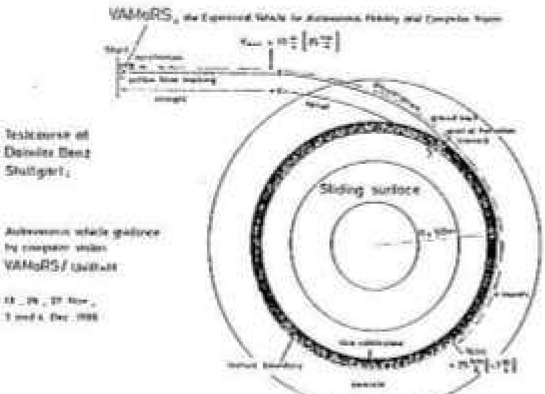

Fig. 8. Testrun for VaMoRs, the experimental vehicle for autonomous mobility and computer vision

ing while the windows track the line marking laterally and the system steers the vehicle in such a way that the vehicle moves at a preset distance besides the line with its velocity vector tangential to it. As long as the line is straight and the maximum speed set in advance is not yet achieved the vehicle accelerates. When the curve (a tightening spiral) is reached, curvature is estimated, the anticipatory lateral control u_a is computed and speed is adjusted to curvature.

At point E the line marking ends at a borderline between the bright concrete pavement (outer rink) and the dark basalt pavement of the inner rink. The vehicle continues its path following this border-line at a speed of ≈ 25 km/h which corresponds to a lateral acceleration of 1 m/s^2 (0.1 g).

6. CONCLUSION

The capability of real time image sequence processing for guiding high speed road vehicles along well structured roads is becoming a reality. The method derived integrates the evaluation of perspective projection and the control methods using dynamical models to arrive at a system which has been shown to allow autonomous vehicle guidance at high speed with a relatively small set of today's microcomputers.

More computing power will be needed to improve the checking for obstacles and other objects in a less restricted environment. In principle, the vision system considered has the growth potential to allow the devlopment of autonomous vehicles that fit neatly into the traffic system developed up to now for the human driver. A gradual deployment and mixed human and automatic traffic seems to be possible.

Many problems with respect to safety and reliability will have to be solved before practical introduction of such systems is possible, but it seems that technical systems now are on the verge of acquiring the capability of autonomous locomotion by visual feedback, which up to now was essentially limited to biological systems. In order to fully utilize the new potential, (artificial) intelligence-methods will have to be developed which allow these systems to acquire a certain understanding of processes in their environment and to react properly. This is a challenging new step in engineering.

7. REFERENCES

AWS (1986). DARPA's Pilot's Associate Program Provides Development Challenges. Aviation Week & Space Technology, pp. 45-52.

Dickmanns, E.D., Zapp, A. and K.-D. Otto (1984). Ein Simulationskreis zur Entwicklung einer automatischen Fahrzeugführung mit bildhaften und inertialen Signalen. Proc. 2. Symp. Simulationstechnik, Wien, Inf. Fachberichte 39, Springer-Verlag.

Dickmanns, E.D., Zapp, A. (1985). Guiding Land Vehicles along Roadways by Computer Vision. Proc. Congres Automatique 1985, AFCET, Toulouse.

Dickmanns, E.D. (1986a). Computer Vision in Road Vehicles - Chances and Problems. ICTS-Symposium on "Human Factors Technology for Next-Generation Transportation Vehicles". Amalfi, Italy, June 1986, proceedings to appear.

Dickmanns, E.D., Zapp, A. (1986b). A Curvature-based Scheme for Improving Road Vehicle Guidance by Computer Vision . SPIE Conference 727 on "Mobile Robots", Cambridge, Ma., USA.

Drexler, J. (1986). Automatische Querführung eines Fahrzeugs durch Sichtrückkopplung. Diplomarbeit, Lehrstuhl für Flugmechanik und Flugregelung, TU München.

Gennery, D.B. (1977). A stereo vision system for an autonomous vehicle. Proc. 5th IJCAI, Cambridge, Mass., USA.

Giralt, G. (1984). Mobile Robots. In M. Brady, L.A. Gerhardt, H.F. Davidson (eds.): Robotics and Artificial Intelligence, Springer-Verlag.

Graefe, V. (1984). Two Multi-Processor Systems for Low-Level Real-Time Vision. In M. Brady, L.A. Gerhardt, H.F. Davidson (eds.): Robotics and Artificial Intelligence, Springer-Verlag.

IRD (1985)Artificial Intelligence & Robotics in Military and Paramilitary Markets. International Resource Development INC., Report 637, Norwalk, Connecticut.

Kuhnert, K.-D., Zapp, A. (1985). Wissensgesteuerte Bildfolgeauswertung zur automatischen Führung von Straßenfahrzeugen in Echtzeit. Proc. 7th DAGM-Symposium Erlangen, H. Niemann (ed.): Mustererkennung 1985, Informatik-Fachberichte 107, Springer-Verlag.

Mitschke, M. (1982). Dynamik der Kraftfahrzeuge, Band A, Springer-Verlag.

Moravec, H.P. (1980). Obstacle avoidance and navigation in the real world by a seeing robot rover. Stanford AI-Lab., Memo AIM 340.

Strackerjan, B. (1975). Theoretische Untersuchungen des dynamischen Lenkverhaltens von Personenkraftwagen. Automobil-Industrie 3/75, pp. 49-56.

Zapp, A. (1985). Automatische Fahrzeugführung mit Sichtrückkopplung; Erste Fahrversuche mit einer Fernsehkamera als Echtbauteil im Simulationskreis. UniBw München, LRT/WE 13/FB/85-1.